Effects of Temperature on Adsorption of Methanol on Graphitized Thermal Carbon Black: A Computer Simulation and Experimental Study

ARTICLE *in* THE JOURNAL OF PHYSICAL CHEMISTRY C · JULY 2011

Impact Factor: 4.77 · DOI: 10.1021/jp205498p

3 AUTHORS:

Van T Nguyen
University of Queensland
29 PUBLICATIONS **259** CITATIONS
SEE PROFILE

Duong Do
University of Queensland
493 PUBLICATIONS **9,807** CITATIONS
SEE PROFILE

David Nicholson
University of Queensland
294 PUBLICATIONS **4,527** CITATIONS
SEE PROFILE

THE JOURNAL OF PHYSICAL CHEMISTRY C

ARTICLE

pubs.acs.org/JPCC

Effects of Temperature on Adsorption of Methanol on Graphitized Thermal Carbon Black: A Computer Simulation and Experimental Study

Van T. Nguyen, D. D. Do,* and D. Nicholson

School of Chemical Engineering, University of Queensland, St. Lucia, Qld 4072, Australia

J. Jagiello

Micromeritics Instrument Corporation, Norcross, Georgia 30093, United States

ABSTRACT: We report a computer simulation and experimental study of adsorption of methanol on a highly graphitized thermal carbon black over a range of temperatures to investigate the adsorptive capacity, the isosteric heat, and the configuration of molecules in the adsorbed layer. We include coverage beyond the monolayer region, not previously studied in detail. The adsorption is shown to be strongly affected by hydrogen bonding which results in strong fluid−fluid interaction between the adsorbed molecules. The adsorption isotherms are initially sigmoidal, however, and in the multilayer region the isotherms follow typical type II behavior. The isosteric heat of adsorption of methanol is distinctly different from that of simple gases because of the dominance of the strong interactions between adsorbed molecules over the solid−fluid interactions. The configuration of adsorbed molecules in the submonolayer region favors the formation of 2D cyclic clusters of four or five methanol molecules, which maximizes the hydrogen bonding, while near the end of the completion of the first layer methanol molecules form molecular chains with some degree of 2D-zigzag pattern which again maximizes the hydrogen bonding between all molecules. This is in qualitative agreement with the X-ray diffraction measurements obtained by Morishige (Morishige, K.; Kawamura, K.; Kose, A. *J. Chem. Phys.* **1990**, *93*, 5267). When the second and higher layers are formed above the surface, the adsorbate forms clusters in three-dimensional configurations; however, the molecular chains with some degree of 2D-zigzag pattern in the first layer still remain.

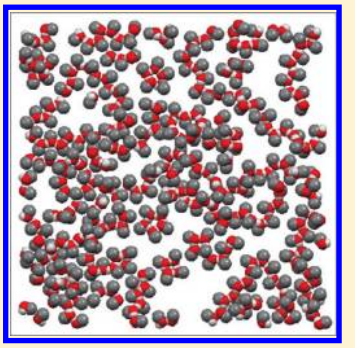

1. INTRODUCTION

Adsorption of methanol on carbon black and graphite surfaces has been studied experimentally by a number of workers[2−7] mainly because of the interest in understanding how associating fluids interact with a basal plane of graphite. However, in many of these publications, the adsorbent is heterogeneous, and the interaction of methanol with the substrate is dominated by defects and functional groups as reflected in the high initial heat of adsorption which then decreases with loading when the adsorption occurs on progressively weaker sites, the characteristic signature of a heterogeneous surface. In a few studies, notably those by Kiselev and co-workers,[8−10] adsorption and isosteric heat were measured on highly homogeneous surfaces, but unfortunately their data are limited to a monolayer. The configuration of a crystalline monolayer of adsorbed methanol on graphite has been studied by Morishige over a temperature range 30−215 K,[1] and like Kiselev he was interested mainly in the behavior of a single layer of adsorbed molecules over the graphite surface. Likewise, the molecular simulation work of Birkett and Do[11] is also restricted to submonolayer coverage.

In this work, we address a fundamental question of methanol behavior when adsorption occurs beyond the monolayer coverage by carrying out a detailed computer simulation and experimental measurement of methanol on a very homogeneous carbon black, Carbopack F, over a wide range of temperatures. The computer simulation was performed in the Grand Canonical Monte Carlo (μ,V,T).[12] The aggregation volume-bias (AVB) algorithm proposed by Chen and Siepmann[13,14] was implemented to enhance the frequency of sampling of formation and destruction of bonded configurations. Due to the strong fluid−fluid interaction between methanol molecules, the Markov chain of the Monte Carlo simulation is likely to be temporarily trapped in metastable states. Therefore, much longer cycles are required for simulation of methanol adsorption in comparison with simple molecules such as argon.

In the experimental study, we use a highly graphitized thermal carbon black, Carbopack F, supplied by Supelco, USA. The particles of this carbon black have a polyhedron shape as shown in the TEM image in Figure 1, and the exposed faces are formed by the basal planes of a graphene layer. The adsorption isotherm measurements were carried out with the Micromeritics ASAP-2020 connected to a Cryo-pump which allows us to control the

Received: June 12, 2011
Revised: July 14, 2011
Published: July 19, 2011

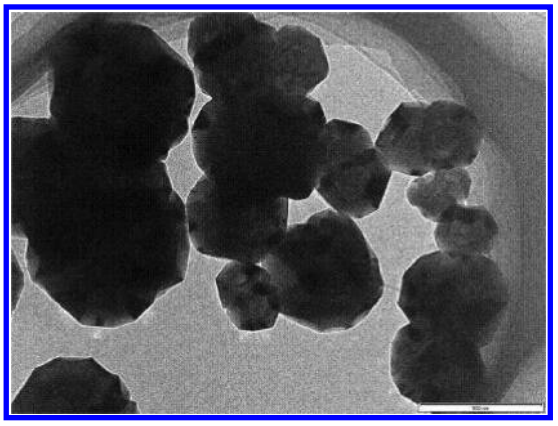

Figure 1. TEM of Carbopack F.

Table 1. Molecular Parameters of the TraPPE Model of Methanol

parameters	units	methanol
σ of CH_3	nm	0.375
ε/k_b of CH_3	K	98.0
σ of O	nm	0.302
ε/k_b of O	K	93.0
q of CH_3	e	0.265
q of O	e	−0.700
q of H	e	0.435
R_{C-O}	nm	0.1430
R_{O-H}	nm	0.0945
angle COH	°	108.5

adsorption temperature accurately to ±0.2 K. Comparison between the experimental measurements at various temperatures and the computer simulations will provide insight into how methanol and other associating fluids adsorb on graphitic surfaces. This is the main objective of this work.

2. THEORY

2.1. Fluid−Fluid Potential Energy. Methanol is treated as a rigid molecule with Lennard-Jones sites and fixed partial charges. The hydrogen bonding is represented by the Coulombic component of the fluid−fluid interaction. The intermolecular interaction energy between a molecule i and a molecule j, $\varphi_{i,j}$, is described by the following equation

$$\varphi_{i,j} = 4\sum_{\alpha=1}^{A}\sum_{\beta=1}^{B}\varepsilon_{i,j}^{\alpha,\beta}\left[\left(\frac{\sigma_{i,j}^{\alpha,\beta}}{r_{i,j}^{\alpha,\beta}}\right)^{12} - \left(\frac{\sigma_{i,j}^{\alpha,\beta}}{r_{i,j}^{\alpha,\beta}}\right)^{6}\right] + \frac{1}{4\pi\varepsilon_0}\sum_{a=1}^{A}\sum_{b=1}^{B}\frac{q_i^a q_j^b}{r_{i,j}^{a,b}} \quad (1)$$

where the variable or parameter $X_{i,j}^{\alpha,\beta}$ is associated with site α on molecule i and site β on molecule j. The parameters $\sigma_{i,j}^{\alpha,\beta}$ and $\varepsilon_{i,j}^{\alpha,\beta}$ are the cross collision diameter and the cross well depth of interaction energy, respectively, and are calculated from the

Table 2. Saturation Properties of the Methanol Model for a Number of Temperatures from GEMC

parameter	units	300 K	316 K	326 K
P^{VAP}	kPa	16.9	40.4	60.0
ρ^V	mol/m^3	8.4	21.4	26.36
ρ^L	kmol/m^3	24.1	22.3	20.12
ΔH^V	kJ/mol	38.6	37.5	36.9

Table 3. Experimental Vapor Pressure of Methanol at Temperatures Studied

parameter	units	254.35 K	263.15 K	273.15 K	283.15 K	293.15 K
P^{VAP}	kPa	1.111	2.080	4.017	7.374	12.927

Lorentz−Berthelot rule

$$\sigma_{i,j}^{\alpha,\beta} = (\sigma_i^{\alpha} + \sigma_j^{\beta})/2 \qquad \varepsilon_{i,j}^{\alpha,\beta} = \sqrt{(\varepsilon_i^{\alpha}\varepsilon_j^{\beta})} \quad (2)$$

The parameter q_i^{α} is the charge on the site α of the molecule i, and ε_0 is the permittivity of a vacuum.

Several potential models for methanol have been proposed in the literature.[15,16] Here we have used the TraPPE potential model[16] as it gives a good account of the vapor−liquid equilibrium. This model belongs to the United Atom family because it treats the methyl group as one site; the parameters of this model are listed in Table 1. The model has two L-J sites, on the methyl group and on the oxygen atom, and three fixed partial charges, on the methyl group, on the oxygen atom, and on the hydrogen atom.

Using this TraPPE model in the Gibbs Ensemble Monte Carlo simulation, we have obtained the vapor−liquid properties for methanol given in Table 2 for three temperatures. To calculate the vapor pressure at lower temperatures, we used the Antoine equation $\ln(P_0) = B - A/T$ to fit the GEMC data in Table 2 and extrapolated the results (Table 3).

2.2. Solid Surface and Solid−Fluid Potential Energy. The graphite was modeled as a homogeneous solid, constructed from graphene layers. Corrugation of the surface potential and the electric field due to quadrupoles in the basal plane were neglected because the carbon−carbon bond length in the basal plane, 0.142 nm, is smaller than the collision diameter of any site in the methanol molecule. The interaction of the quadrupoles with the electrostatic sites in the methanol does not affect the holding potential, and the contribution to the repulsion between methanol molecules from induced dipoles is extremely small compared to the L-J and electrostatic interactions. Therefore, the solid−fluid potential energy of the L-J site α in a methanol molecule i and the surface can be calculated by the Steele 10-4-3 potential equation[17]

$$\varphi_{i,S}^{\alpha} = 2\pi\rho_s(\sigma_{i,S}^{\alpha,C})^2\varepsilon_{i,S}^{\alpha,C}\left[\frac{2}{5}\left(\frac{\sigma_{i,S}^{\alpha,C}}{z_i^{\alpha}}\right)^{10} - \left(\frac{\sigma_{i,S}^{\alpha,C}}{z_i^{\alpha}}\right)^{4} - \frac{(\sigma_{i,S}^{\alpha,C})^4}{3\Delta(z_i^{\alpha} + 0.61\Delta)^3}\right] \quad (3)$$

in which the subscript S denotes the graphite surface and superscript C the carbon atom. The parameter Δ is the spacing

dx.doi.org/10.1021/jp205498p |J. Phys. Chem. C 2011, 115, 16142–16149

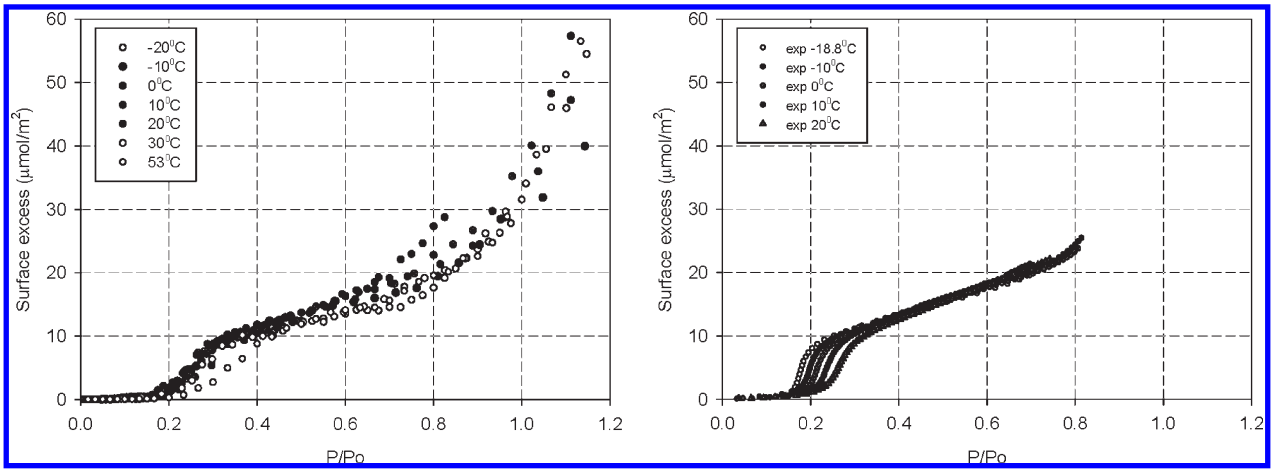

Figure 2. Isotherms for methanol adsorption on Carbopack F at various temperatures: (a) simulation results and (b) experimental data from Micromeritics company.

between two adjacent graphene layers (0.335 nm), and ρ_s is the carbon surface density of the graphene layer (38.2 nm^{-2}).

The carbon surface is positioned on one face of the simulation box normal to the z-direction. The box height is chosen large enough that the opposite face can be modeled as a hard wall. Periodic boundary conditions are imposed on the boundaries in the x- and y-directions. The GCMC simulation gives the number of molecules and the isosteric heat which can be obtained directly from the fluctuation formula[18]

$$q_{st} = -\frac{\langle NU\rangle - \langle N\rangle\langle U\rangle}{\langle N^2\rangle - \langle N\rangle\langle N\rangle} + kT \qquad (4)$$

This equation is valid only when the gas behaves as an ideal gas. A more exact equation for nonideal gases is given by Do et al.[19] Equation 4 can be split into two contributions, one from the fluid−fluid interaction and the other from the solid−fluid interaction, which allow us to study the relative contributions from these interactions.

2.3. Experimental Procedure. The carbon used in this work is a highly graphitized thermal carbon black, Carbopack F. Before each experiment, the sample was pretreated overnight under a vacuum 1×10^{-3} Pa at 300 °C. Adsorption isotherms were measured with a high-resolution apparatus ASAP 2020 (Micromeritics company in Norcross, Georgia, USA). This apparatus has chemically resistant Kalrez seals and a heated manifold and is equipped with three accurate pressure transducers, 0.0133, 1.33, and 133 kPa at full scale, which allow us to obtain isotherm data at extremely low pressures as well as pressures up to 1 atm. The temperature is accurately controlled by a refrigerated/heating circulator (Julabo F33) with the temperature stability of ±0.03 °C which is capable of controlling temperatures from −30 to 80 °C.

3. RESULTS AND DISCUSSION

3.1. Adsorption Isotherms. The results of the simulations on Carbopack F at various temperatures are presented in Figure 2a and compared with experimental data obtained by Micromeritics (Figure 2b). Since the vapor pressure of the methanol model is not exactly the same as the experimental vapor pressure, we present these plots in terms of the reduced pressure; i.e., the pressure in the molecular simulation is scaled by the vapor

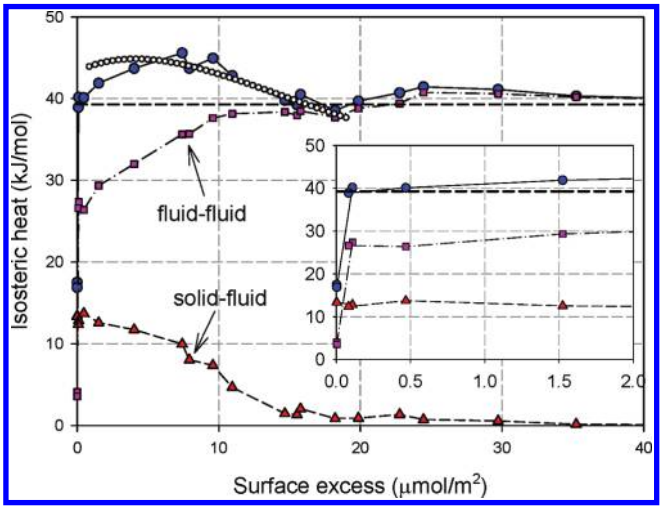

Figure 3. Heat of adsorption and its contributions for methanol adsorption on carbon black at 0 °C: total heat (filled circles), contribution from solid−fluid interaction (triangles), and contribution from fluid−fluid interaction (squares). Horizontal dashed line indicates the heat of condensation. Unfilled circles represent isosteric heat obtained from a virial-type thermal adsorption equation.[21]

pressure obtained from the Gibbs ensemble MC. These simulation results show good qualitative agreement with the experimental data and capture the essential features of the experimental isotherms, especially the initial sigmoid shape and the gradual increase in coverage above the transition to the monolayer. We note that the adsorption capacity is negligible at low relative pressures due to the fact that the fluid−fluid interaction is more dominant than the solid−fluid interactions. This is generally the case for associating fluids such as methanol, ammonia, and water which show weak adsorption at low pressures. As pressure is increased, the adsorption uptake increases rapidly as the methanol molecules start to form separated clusters on the surface. This uptake is steeper for lower temperatures where it occurs at a lower reduced pressure, and the consequent separation in the isotherms in this region is particularly notable in the experimental data. This form of isotherm is in good agreement with the results obtained by Kiselev et al.[8,10] who measured isotherms of

methanol on a highly graphitized thermal carbon black by a gas chromatographic method and noted their unusual form which is not included in IUPAC classification.[20] These isotherms are initially of type III (convex to the pressure axis) and then become concave and change to a type II at higher coverage. We also note that over the whole temperature range from the monolayer coverage onward the experimental isotherms are very nearly superimposed up to the maximum relative pressure of 0.8; the simulated isotherms show a slightly wider divergence in this range. This is explained by the dominance of the fluid−fluid interaction compared to the nearly negligible interaction of the methyl group with the graphite surface beyond the monolayer coverage.

3.2. Isosteric Heat. Figure 3 shows the simulated heat of adsorption versus loading at 0 °C (filled circles). The heat curve can be decomposed into contributions from solid−fluid and fluid−fluid interactions, also shown in Figure 3 as filled triangles and squares, respectively. Initially the solid−fluid interactions make a significant contribution to the total heat. This contribution quickly decreases and becomes negligible when the coverage approaches two layers; beyond this point, adsorption is primarily a process of condensation onto the already adsorbed film.

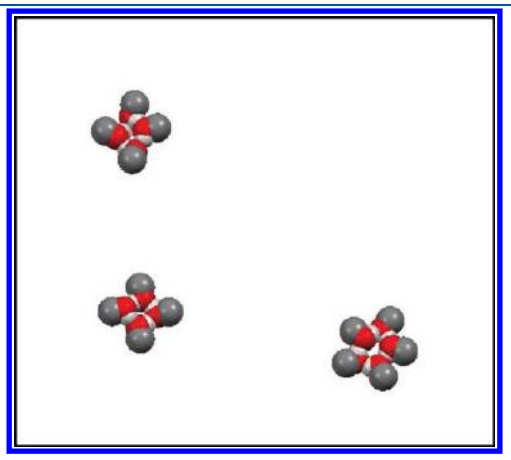

Figure 4. Snapshots of methanol on carbon black at 0 °C at reduced pressure of 0.17. Different groups are represented: CH_3 (gray), O (red), H (white).

The inset in Figure 3 shows that the heats of methanol adsorption at zero loading are much lower than the heat of condensation because the solid−fluid interaction is less than the fluid−fluid interaction in the bulk liquid phase. However, the isosteric heat increases quickly and approaches the condensation heat at a loading well below the monolayer coverage. This suggests that methanol molecules interact specifically to form clusters by hydrogen bonding whose energy is added to the small value of adsorbate−adsorbent interaction energy, thus causing a rapid rise in the heat of adsorption. These results are in good agreement with those reported for methanol adsorption on carbon black by Kiselev et al.[8]

After the heat of condensation has been reached, the isosteric heat passes through maximum, partly due to the contribution from the solid−fluid interaction and partly from the increasing fluid−fluid contribution. The isosteric heat then decreases to the condensation heat at a surface excess of approximately 20 μmol/m^2 (about two times the statistical monolayer coverage). At higher coverage where the contribution from solid−fluid interactions becomes negligible, the isosteric heat approaches the heat of condensation and remains unchanged through multilayer coverage.

Interestingly, it can be seen from Figure 3 that the simulated isosteric heat is in good agreement with that calculated from a virial-type thermal adsorption isotherm developed by Jagiello et al.[21]

$$\ln(p) = \ln(v) + \frac{1}{T}\sum_{i=0}^{m} a_i v^i + \sum_{i=0}^{n} b_i v^i \quad (5)$$

where v, p, and T are the amount adsorbed, pressure, and temperature, respectively, and a_i and b_i are empirical parameters. Parameters a_i and b_i are obtained by fitting this equation to the adsorption data measured at two or more temperatures (Figure 2b). The isosteric heat of adsorption as a function of v is given by

$$Q_{st} = -R\left(\frac{\partial \ln(p)}{\partial(1/T)}\right)_V = -R\sum_{i=0}^{m} a_i v^i \quad (6)$$

where R is the universal gas constant.

3.3. Methanol Configuration. Figure 4 shows a snapshot of methanol on graphite at 0 °C at a reduced pressure of 0.17 before

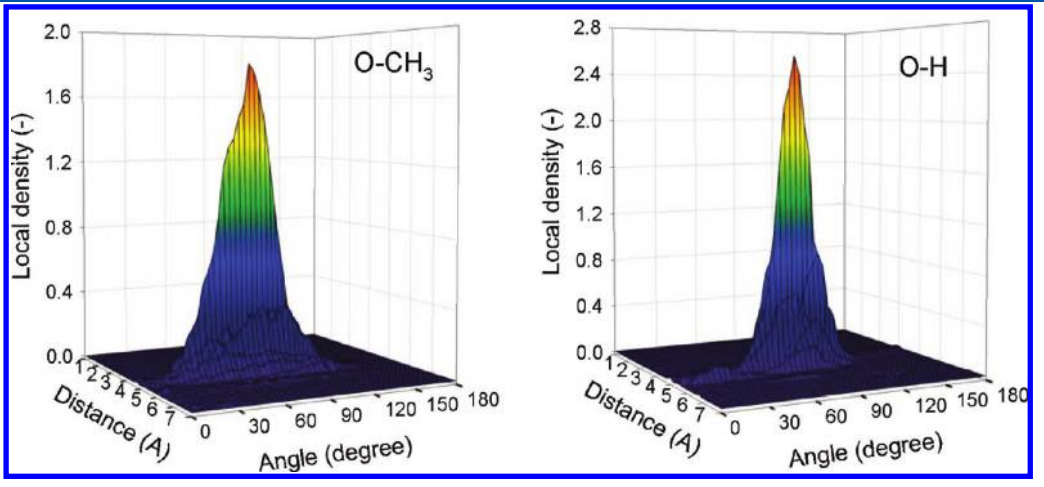

Figure 5. Variation of the 3D orientation-dependent local density versus distance and angle for methanol at 0 °C at reduced pressure of 0.17: (a) orientation of the O−CH_3 bond and (b) orientation of the O−H bond.

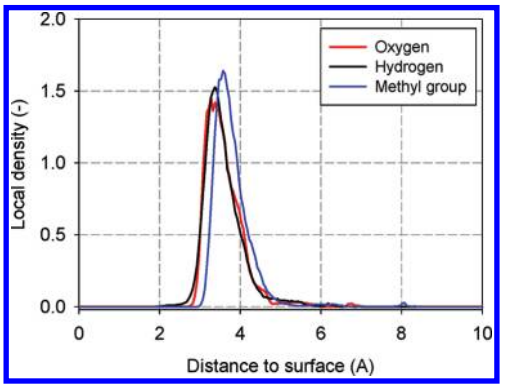

Figure 6. Local density distribution of different groups for methanol at 0 °C at reduced pressure of 0.17.

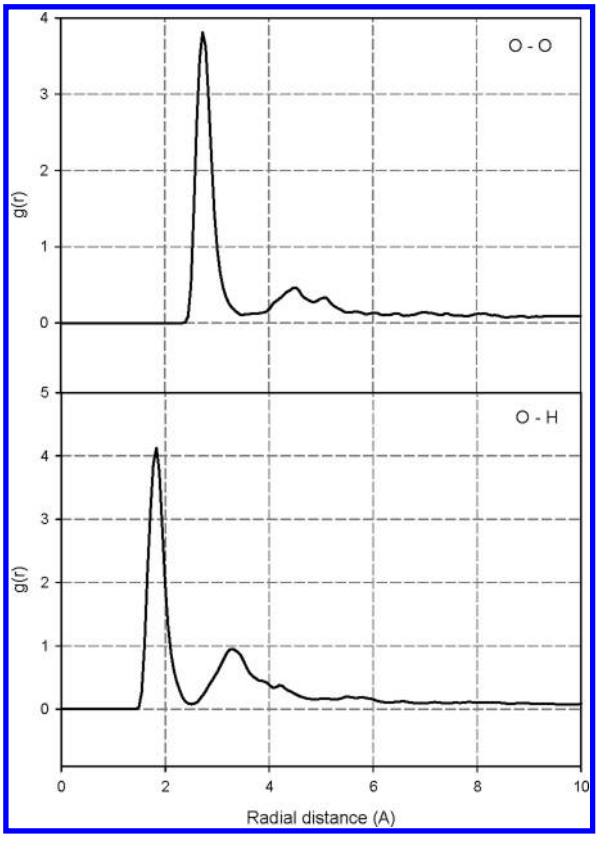

Figure 7. O−O and O−H radial distributions for methanol at 0 °C at reduced pressure of 0.17.

the monolayer transition. At low coverage, methanol molecules form clusters of four or five molecules with the oxygen atom and methyl group lying flat on the surface. The O-atoms are at the vertices, and the H-atoms form the sides of the square or pentagon which optimizes the H-bonding. The coplanar arrangement of the methyl group and oxygen atom is confirmed by the 3D plot of the orientation-dependent density distribution of O−CH_3 and O−H bonds (Figure 5) where the orientation-dependent density is calculated as follows[22]

$$\rho(z,\theta) = \frac{2\langle \Delta N(z,\theta)\rangle}{L_x L_y \Delta z \sin\theta \cdot \Delta\theta} \quad (7)$$

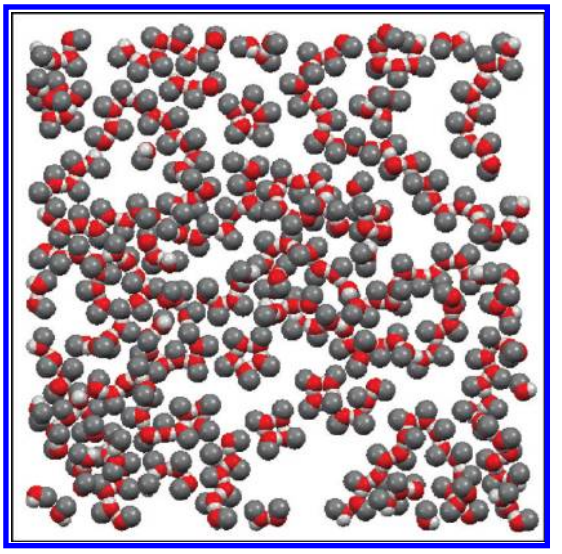

Figure 8. Snapshots of methanol on carbon black at 0 °C at reduced pressure of 0.3. Different groups are represented: CH_3 (gray), O (red), H (white).

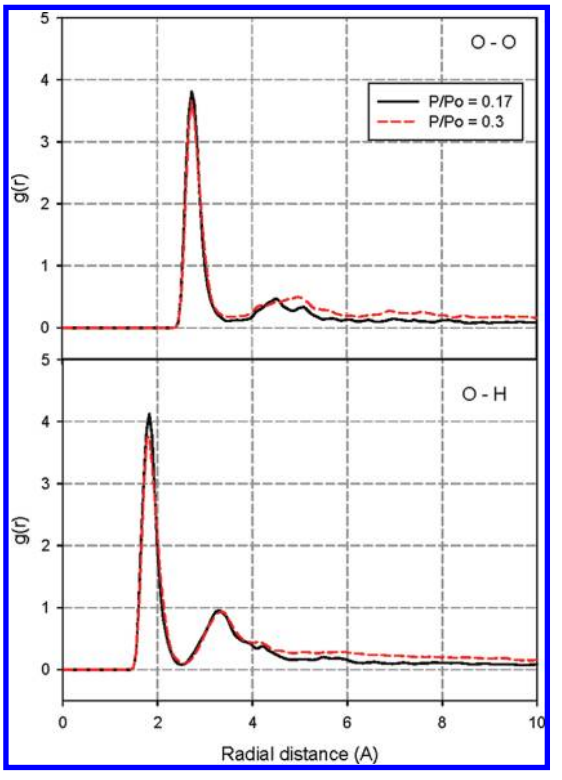

Figure 9. O−O and O−H radial distributions for methanol at 0 °C at reduced pressure of 0.3.

where $\Delta N(z, \theta)$ is the number of methanol molecules whose centers of mass are located in the segment having boundaries z, $z + \Delta z$, and the angle between the z-direction and the O−CH_3 or O−H bond falling between θ, $\theta + \Delta\theta$.

It can be seen from Figure 5a that the peak of the 3D-plot of orientation of the O−CH_3 bond is at an angle less than 90°. Since the collision diameter of the methyl group (0.375 nm) is larger than that of the O-atom (0.3 nm), this peak indicates that

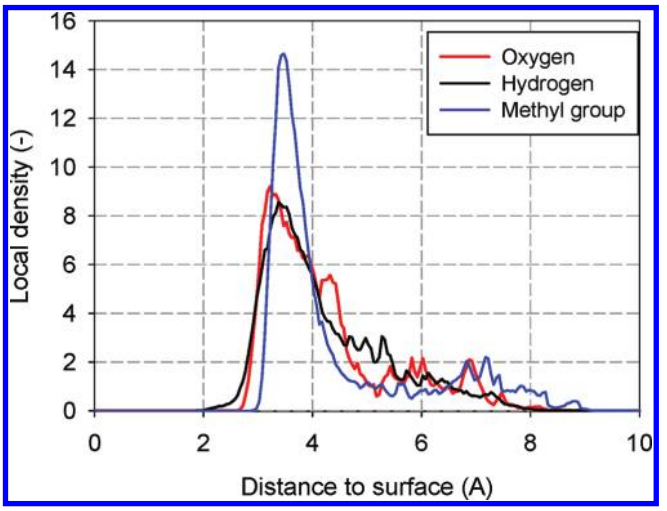

Figure 10. Local density distribution of different groups for methanol at 0 °C at reduced pressure of 0.3.

preferential orientation of methyl groups and O-atoms is on the graphite surface. In contrast, the peak in Figure 5b shows the preferential orientation of the O−H bond at a 90° angle with the *z*-direction, indicating that hydrogen atoms favor a collinear geometry of participating O···H···O. This is confirmed by Figure 6 which shows the local density of O-atoms, H-atoms, and methyl groups as a function of distance to the surface for methanol adsorption at 0 °C at a reduced pressure of 0.17.

From the Lorentz−Berthelot rule (eq 2), we computed $\sigma_{sf}(O) = 0.321$ nm and $\sigma_{sf}(CH_3) = 0.3575$ nm which correspond to the peaks of local density distribution of O-atoms and methyl groups, respectively, in Figure 6. This again confirms that O-atoms and methyl groups are lying flat on the surface. The peak of local density distribution of H-atoms located at the same position with that of O-atoms shows that H-atoms are at the same distance to the surface as oxygen; i.e., the O−H bond is parallel to the surface.

The O−O and O−H radial distributions (Figure 7) obtained from the simulation confirm the tetramer or pentamer formation of methanol on the graphite surface at low surface coverage. The

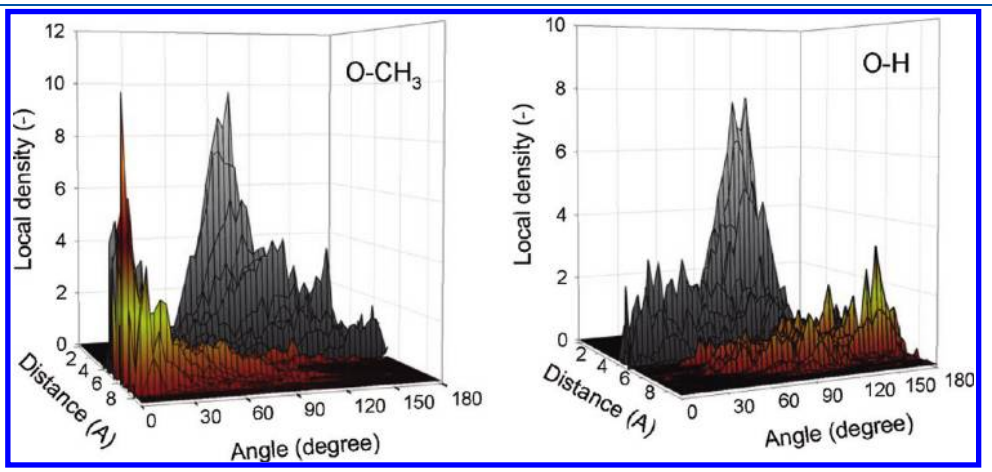

Figure 11. Variation of the 3D orientation-dependent local density versus distance and angle for methanol at 0 °C at reduced pressure of 0.3: (a) orientation of the O−CH_3 bond and (b) orientation of the O−H bond. Different colors are used for clarity: 1st layer, gray; 2nd layer, yellow.

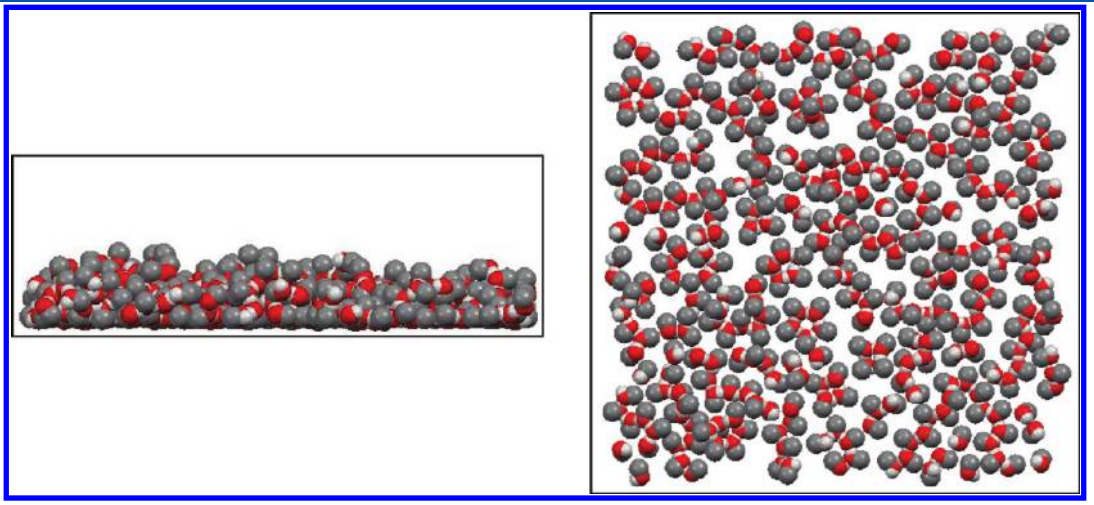

Figure 12. Snapshots of methanol on carbon black at 0 °C at a reduced pressure of 0.67. Different groups are represented: CH_3 (gray), O (red), H (white): (a) whole system (side view) and (b) first layer (top view).

first peaks in O−O radial distribution correspond to the nearest distance between O atoms of two adjacent methanol molecules (~0.3 nm) which are positioned at the side of the square or pentagon. The second maximum corresponds to the next nearest-neighbor O-atoms in a 0.3 nm × 0.3 nm square (0.42 nm), while the third maximum corresponds to the next nearest distance of 0.49 nm in a pentagon.

Near to the completion of the monolayer ($P/P_0 \sim 0.3$), methanol molecules form molecular chains on the surface which maximize the hydrogen bonding between all molecules as shown in Figure 8. Morishige[1] reported the X-ray diffraction measurements for methanol adsorption on graphite over the temperature range 30−215 K, which is much lower than the temperature range studied in this work. The diffraction data of Morishige show that the interactions between the molecule and the surface result in the nearly coplanar arrangement of the carbon and oxygen atoms in the monolayer, whereas the zigzag chains of hydrogen bonds are formed in the crystalline monolayer of methanol on graphite. Our simulation results are in good agreement with Morishige's data. From Figure 8 we observe that methanol molecules form molecular chains with some degree of zigzag pattern; however, at 273 K, methanol molecules are more loosely packed than that observed by Morishige at lower temperatures due to thermal motion of molecules, and therefore some clusters of tetramer and pentamer still exist in the snapshot (Figure 8).

The radial distributions show (Figure 9) that the second maximum of the O−O radial distribution is shifted to the right and becomes more delocalized, indicating that the 2D-cyclic rings of four or five methanol molecules on the surface are disrupted.

Due to thermal motion of methanol molecules at 273 K, the second layer starts to form while the first layer has not been completed yet. By observing Figure 8, we can see some O-atoms and H-atoms of the first layer standing off the surface to form hydrogen bonding with methanol molecules in the second layer. This is confirmed by the local density distribution of different groups shown in Figure 10. It is seen that the distributions of O-atoms and H-atoms become broader. Their peaks are lower than that of the methyl group, whereas methyl groups prefer to position on the surface due to the LJ interactions between methyl groups and the solid surface.

The 3D orientation-dependent local density distribution of O−CH_3 and O−H bonds for methanol adsorption at 0 °C at reduced pressure of 0.3 is shown in Figure 11. We see from Figure 11 that there is a small population of O-atoms and H-atoms of the first layer standing off the surface. Besides, we do not observe coplanar arrangement of methyl groups and O-atoms in the second layer as what was observed in the monolayer since the O−CH_3 bonds tend to be oriented normal to the surface.

As adsorption progresses beyond a monolayer, the methanol molecules form three-dimensional clusters as shown in Figure 12. As a result of the growth of methanol clusters due to hydrogen bonding, we observe a type II gradual increase in the amount adsorbed as we have discussed above (section 3.1).

Figure 12b shows the snapshot of the first layer at relative pressure of 0.67 which is found not to be much different from that observed at lower pressure (Figure 8). This is confirmed by observing the O−O and O−H radial distributions of methanol adsorbed in the first layer at reduced pressures of 0.3 and 0.67 (Figure 13). It can be seen that although there is some fluctuation in the radial distributions beyond the radial distance of 4 A, the shape of $g(r)$ remains almost unchanged as pressure is increased.

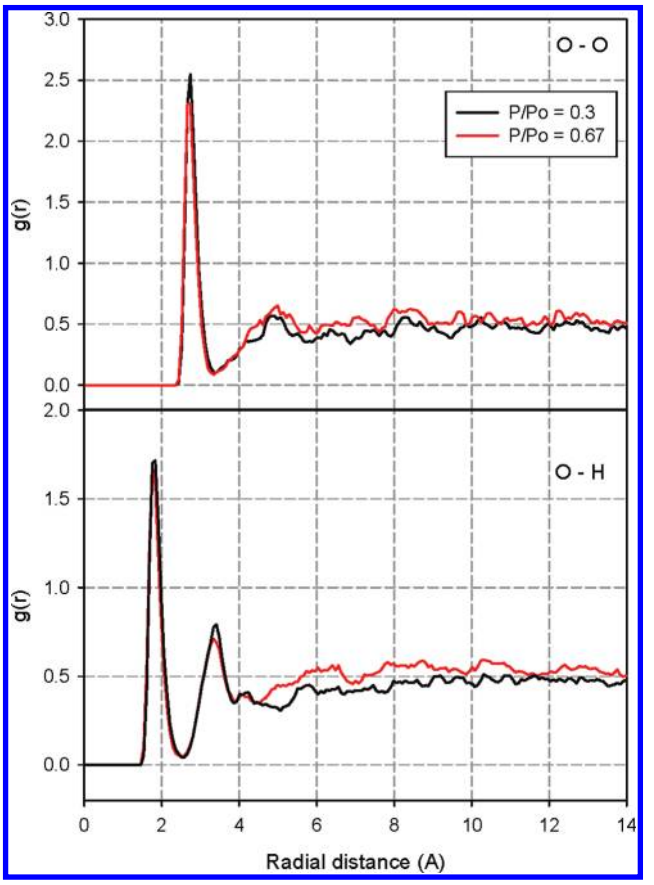

Figure 13. O−O and O−H radial distributions for the 1st layer of methanol at 0 °C at reduced pressure of 0.3 and 0.67.

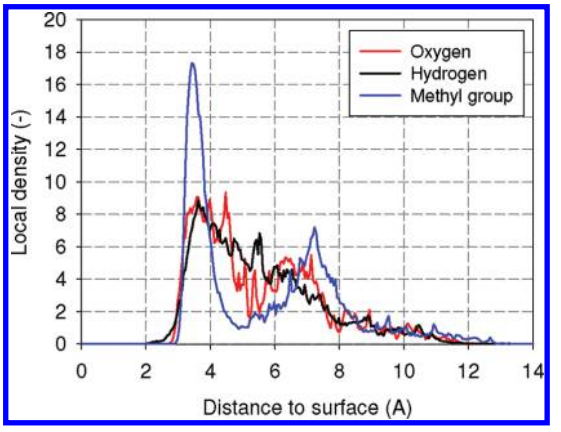

Figure 14. Local density distribution of different groups for methanol at 0 °C at reduced pressure of 0.67.

This suggests that the molecular chains with some degree of 2D zigzag pattern are not much perturbed by the presence of higher layers.

The 3D growth of methanol clusters is also confirmed by observing the local density distributions (Figure 14) which show broader distributions of O-atoms and H-atoms. This indicates that as loading increases there are more O-atoms and H-atoms standing off to form hydrogen bonding with molecules in the second layer.

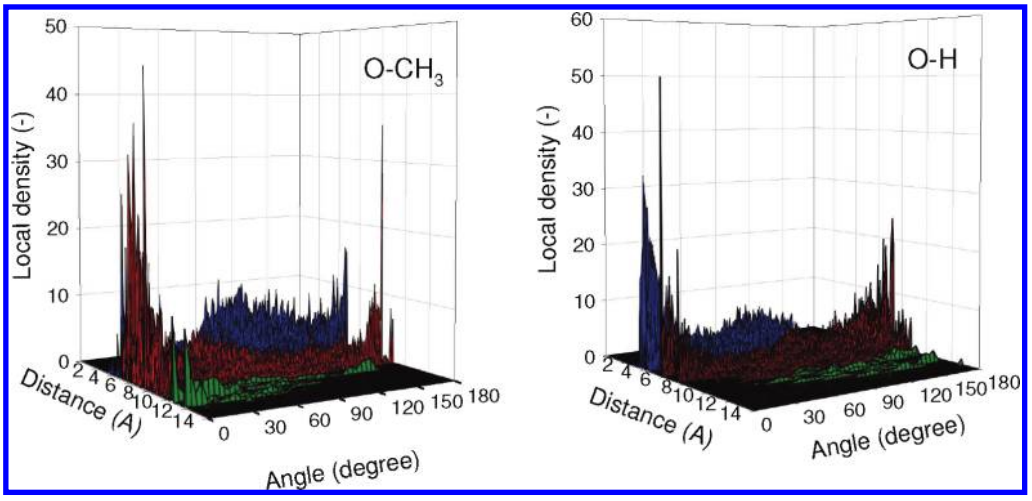

Figure 15. Variation of the 3D orientation-dependent local density versus distance and angle for methanol at 0 °C at reduced pressure of 0.67: (a) orientation of the O−CH_3 bond and (b) orientation of the O−H bond. Different colors are used for clarity: 1st layer, blue; 2nd layer, red; 3rd layer, green.

On the observation of the 3D orientation-dependent local density distribution of O−CH_3 and O−H bonds for methanol adsorption at 0 °C at reduced pressure of 0.67 (Figure 15), there is more population of O−CH_3 and O−H in the first layer oriented normally to the surface in comparison with that at lower loading. Besides, we observe that in the second and higher layers the coplanar arrangement of O-atoms and methyl groups no longer exists. From Figure 15 it can be seen that O−CH_3 and O−H bonds of second and higher layers have preferential orientation parallel to the *z*-direction.

4. CONCLUSION

Monte Carlo simulations and experiments have been carried out to study adsorption of methanol on highly graphitized carbon black, Carbopack F, at various temperatures. A qualitative agreement between computer simulations and experimental study was obtained. It was found that due to the dominance of H-bonded fluid−fluid interaction over the solid−fluid interaction adsorption isotherms, isosteric heats, and configurations of methanol molecules show similar behavior over the range of temperature studied. Up to monolayer coverage, adsorption isotherms of methanol on Carbopack F exhibit type III character but become type II in the multilayer region. The isosteric heat shows a shallow maximum at low loading, in agreement with calculations from the experimental data because adsorbate interactions initially increase more rapidly than the decrease in adsorbate−adsorbent interactions; it then approaches the heat of condensation at loadings below the monolayer coverage. At low loading, the methanol molecules form tetramers or pentamers lying flat on the surface, while at loadings near the completion of the monolayer they form molecular chains to maximize the hydrogen bonding between all molecules. However, this configuration is not perturbed much by the formation of three-dimensional methanol clusters when the second and higher layers are formed.

AUTHOR INFORMATION

Corresponding Author

*E-mail: d.d.do@uq.edu.au.

ACKNOWLEDGMENT

This project is supported by the Australian Research Council. J.J. would like to acknowledge Amanda Thomson, Micromeritics Analytical Services, for performing adsorption measurements.

REFERENCES

(1) Morishige, K.; Kawamura, K.; Kose, A. *J. Chem. Phys.* **1990**, *93*, 5267.
(2) Pierce, C.; Smith, R. N. *J. Phys. Colloid Chem.* **1950**, *54*, 354.
(3) Millard, B.; Beebe, R. A.; Cynarski, J. *J. Phys. Chem.* **1954**, *58*, 468.
(4) Berezin, G. I.; Kiselev, A. V.; Kleshnin, I. V. *Russ. J. Phys. Chem.* **1969**, *43*, 1657.
(5) Kowalczyk, H.; Rychlicki, G.; Terzyk, A. P. *Pol. J. Chem.* **1993**, *67*, 2019.
(6) Carrott, P. J. M.; Ribeiro Carrott, M. M. L.; Cansado, I. P. P. *Carbon* **2001**, *39*, 193.
(7) Andreu, A.; Stoeckli, H. F.; Bradley, R. H. *Carbon* **2007**, *45*, 1854.
(8) Avgul, N. N.; Kiselev, A. V. *Chem. Phys. Carbon* **1970**, *6*, 1.
(9) Belyakova, L. D.; Kovaleva, N. V.; Kiselev, A. V. *Anal. Chem.* **1964**, *36*, 1517.
(10) Belyakova, L. D.; Kiselev, A. V.; Kovaleva, N. V. *Russ. J. Phys. Chem., USSR* **1968**, *42*, 1204.
(11) Birkett, G. R.; Do, D. D. *Mol. Simul.* **2006**, *32*, 887.
(12) Metropolis, N.; Rosenbluth, A. W.; Rosenbluth, M. N.; Teller, A. H. *J. Chem. Phys.* **1953**, *21*, 1087.
(13) Chen, B.; Stubbs, J. M.; Siepmann, J. I. *Abstr. Pap. Am. Chem. Soc.* **2001**, *221*, 251.
(14) Chen, B.; Siepmann, J. I. *J. Phys. Chem. B* **2001**, *105*, 11275.
(15) Jorgensen, W. L. *J. Phys. Chem.* **1986**, *90*, 1276.
(16) Chen, B.; Potoff, J.; Siepmann, I. *J. Phys. Chem. B* **2001**, *105*, 3093.
(17) Steele, W. A. *Surf. Sci.* **1973**, *36*, 317.
(18) Nicholson, D.; Parsonage, G. *Computer Simulation and the Statistical Mechanics of Adsorption*; Academic Press: London, 1982.
(19) Do, D. D.; Do, H. D.; Nicholson, D. *J. Phys. Chem. B* **2009**, *113*, 1030.
(20) *Pure Appl. Chem* **1985**, *57*, 603.
(21) Czepirski, L.; Jagiello, J. *Chem. Eng. Sci.* **1989**, *44*, 797.
(22) Klochko, A. V.; Brodskaya, E. N.; Piotrovskaya, E. M. *Langmuir* **1999**, *15*, 545.